



Theoretical analysis of different membrane distillation modules

Jaewuk Koo^a, Sangho Lee^{a,*}, June-Seok Choi^b, Tae-Mun Hwang^b

^aSchool of Civil and Environmental Engineering, Kookmin University, Jeongneung-Dong, Seongbuk-Gu, Seoul 136-702, Republic of Korea, Tel. +82 2 910 4529; Fax: +82 2 910 4939; emails: koojaewuk@naver.com (J. Koo), sanghlee@kookmin.ac.kr (S. Lee)

^bDepartment of Construction Environmental Research, Korea Institute of Construction Technology, 2311 Daehwa-Dong, Ilasan-gu, Kyonggi-do, Republic of Korea, emails: jschoi@kict.re.kr (J.-S. Choi), taemun@kict.re.kr (T.-M. Hwang)

Received 26 January 2014; Accepted 16 May 2014

ABSTRACT

Membrane distillation (MD) is a thermally driven separation process that uses hydrophobic membranes. Although MD has been considered as an alternative desalination technology, relatively little information is available on the design and optimization of MD modules. Accordingly, this study focused on the comparison of various MD modules and the optimization of their operation conditions. Direct contact MD, air gap MD, and vacuum MD were experimentally compared using laboratory-scale systems. Then, the results were theoretically analyzed using a simple transport model. Different mass transfer mechanisms inside the membrane were considered in the model, including molecular diffusion, the Knudsen diffusion, and viscous flow. Experimental results showed that the temperature dependences of MD modules were different. This suggests that the optimum feed temperature should be different for each MD module. The dominant mass transfer mechanisms were also identified using the theoretical model for better understanding the characteristics of the MD modules.

Keywords: Membrane distillation; Membrane module; Direct contact membrane distillation; Air gap membrane distillation; Vacuum membrane distillation; Model; Mass transfer mechanism

1. Introduction

Membrane distillation (MD) is a novel desalination technology, which has potential as a cost-efficient alternative to the existing desalination technologies including multi-stage flash distillation and reverse osmosis [1–3]. The driving force for MD is vapor

pressure difference across a porous hydrophobic membrane [4,5]. MD can be operated under relatively low temperature conditions ranging from 50 to 80°C [6], allowing the use of solar thermal energy or waste heat [7,8]. MD also has other attractive features, including high rejection of most inorganic ions (over 99.9%); and capability of high recovery ratio (over 50%) [2,9].

*Corresponding author.

Presented at the 6th International Conference on the “Challenges in Environmental Science and Engineering” (CESE-2013), 29 October–2 November 2013, Daegu, Korea

Generally, MD can be divided into the following configurations, based on the different methods to create a vapor pressure difference across the membrane [5]: (a) direct contact membrane distillation (DCMD) [10]; (b) air gap membrane distillation (AGMD) [11]; (c) sweeping gas membrane distillation (SGMD) [12]; and (d) vacuum membrane distillation (VMD) [13]. In DCMD, the cooling solution directly contacts the permeating side of the membrane. In AGMD, the permeated water vapor, after passing through the air gap in the module, is condensed on a cooling plate inside the module. In SGMD, a sweeping gas drives the water vapor that condensates outside the system. In VMD, vacuum carries the water vapor out of the system and condensation occurs outside the module using additional condenser.

MD process involves simultaneous heat and mass transfers from the feed side, across the boundary layer, and membrane, to the permeate side. Accordingly, there are a lot of factors affecting the performance of MD. For example, the hydrophobicity, pore size, and thermal conductivity of membranes are important in determining the MD configurations [5,14]. Operating parameters such as flow rate, temperature difference, and vapor pressure difference are also important [9,12,15,16]. Unlike pressure-driven membrane processes, not only concentration polarization but also temperature polarization should be considered in MD [2]. Membrane fouling and pore wetting, which are closely related to membrane characteristics and operating conditions, are key issues to successful application of MD [3].

Thus, it is difficult to design an optimum MD module because both thermal and hydrodynamic effects play an important role [17,18]. Accordingly, this study aims at the analysis of different MD modules for better understanding of characteristics of MD modules. DCMD, AGMD, and VMD were experimentally compared using lab-scale MD systems. A simple model considering different transport mechanisms was developed and applied. The dominant transport mechanism and the loss of mass transfer rate were identified using the model.

2. Experimental method

2.1. Membrane

A commercially available hydrophobic PVDF (Polyvinylidene fluoride) membrane (Millipore, USA) was used. Table 1 summarizes the basic properties of the membrane.

2.2. MD test

Three laboratory-scale test systems for DCMD, AGMD, and VMD modules were developed for the experimental study. The basic concepts for the three modules are shown in Fig. 1. The schematic diagrams for the modules are also shown in Fig. 2. Each system has a flat sheet module of same membrane area. In DCMD configuration (Fig. 2(a)), the hot solution (feed) was supplied to directly contact the hot membrane side surface using a gear pump. The vapor was moved by the pressure difference across the membrane to the permeate side and condensed inside the membrane module. An electronic balance connected to a data logger was used to continuously measure water flux through the membrane. In AGMD configuration (Fig. 2(b)), the vapor was moved by the pressure difference across the membrane to the air gap of permeate side and condensed cold surface inside the membrane module. The range of air gap length could be adjusted between 1 and 4 mm. An electronic balance connected to a data logger was used to continuously measure water flux through the membrane. In VMD configuration (Fig. 2(c)), a vacuum pump was used to create a vacuum in the permeate membrane side. The range of vacuum was between 3 and 100 mbar. The vapor passing through the membrane was condensed in the cold trap and collected in the permeate tank, where an electronic balance was connected to measure the flux.

In each system, the temperature of feed was controlled using a heater which is connected to a temperature sensor. It was constantly maintained by a feedback control system. The temperature of distillate in DCMD was controlled by using a water bath and a

Table 1
Property of the MD membrane

Membrane	Nominal pore size (μm)	Effective area (cm^2)	Membrane type	Surface property	Contact angle ($^\circ$)	Porosity (%)
Millipore PVDF	0.22	12.2	flat-sheet	Hydrophobic	145	75

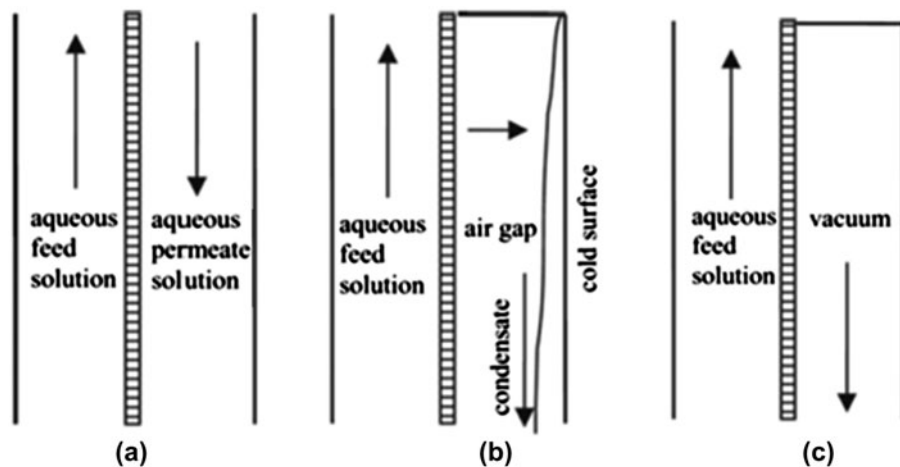


Fig. 1. Basic concept for MD modules (a) DCMD, (b) AGMD, and (c) VMD.

heat exchanger. The temperature of cooling plate in AGMD and vapor condenser in VMD was also controlled using water baths. The recirculation flow rates and feed temperatures were adjusted to 24 L/h and from 40 to 70 °C.

Experiments were carried out using same MD membranes in different MD systems. The operation conditions were adjusted to be similar. Detailed operating conditions are summarized in Table 2.

3. Results and discussion

3.1. DCMD

To begin, a set of fundamental tests was performed in the DCMD system under different conditions. Fig. 3 shows the dependence of flux through the MD membrane on time at various feed temperatures in the DCMD system. The permeate temperature was constant at 20 °C, allowing the temperature difference between 20 and 50 °C. The flow rates for feed and permeate were 24 L/h. As expected, the MD flux increases with increasing feed temperature due to an increased vapor pressure difference. At the feed temperature of 70 °C, the average flux was about 20 L/m²-hr, which is almost five times more than the flux at the feed temperature of 40 °C. The NaCl rejection was over 99.9%, indicating that there was no wetting or leakage.

3.2. AGMD

Fig. 4 shows flux as a function of feed temperature in the AGMD system. Although the same membrane was used, the flux in the AGMD was lower than that

in the DCMD even at same feed temperature. This is attributed to an additional mass transfer resistance by air gap [11]. Again, the flux increases with an increase in feed temperature. For example, the flux at 70 °C of feed temperature was about 10 L/m²-hr, which is almost five times more than the flux at the feed temperature of 40 °C. The NaCl rejection was also over 99.9%.

3.3. VMD

Fig. 5 shows the effect of temperature on flux in the VMD system. At 100 mbar vacuum, the flux was negligible when the feed temperature was lower than 50 °C. Above this, the flux was highly dependent on the feed temperature. At 3 mbar vacuum, the flux was much higher than that at 100 mbar. Nevertheless, the flux at 40 °C was still small. These results suggest that the efficiency of VMD is sensitive to feed temperature. Depending on the degree of vacuum, the minimum feed temperature to produce permeate is likely to be determined. The NaCl rejection was also over 99.9%.

3.4. Experimental comparison of MD modules

The driving force in MD is the difference in vapor pressure across the membrane. In DCMD and AGMD, the vapor pressure difference is a function of feed and permeates temperature. In VMD, it is expressed as the difference between vapor pressure of feed and degree of vacuum. The vapor pressure of water is given by:

$$P_w = \exp\left(\frac{a_1}{T} + a_2 + a_3T + a_4T^2 + a_5T^3 + a_6 \ln(T)\right) \quad (1)$$

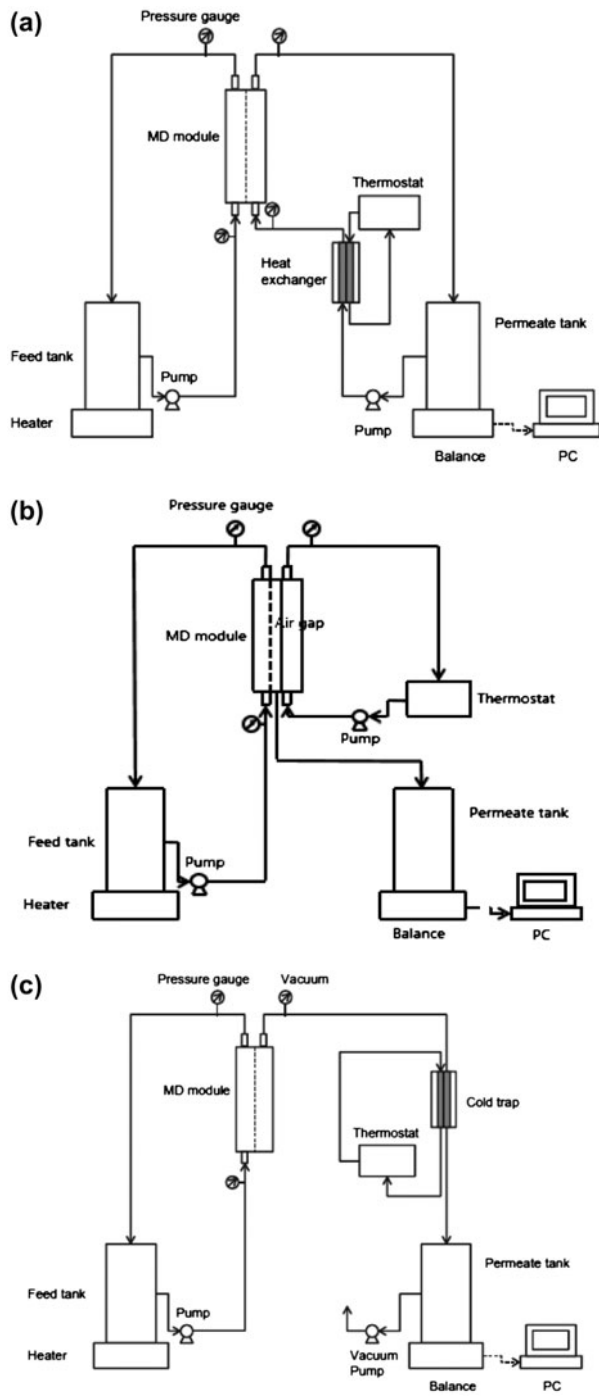


Fig. 2. Schematic diagram of lab-scale MD systems (a) DCMD, (b) AGMD, and (c) VMD.

$$P_v = \frac{P_w}{1 + 0.57357 \frac{C_m}{1000 - C_m}} \quad (2)$$

where P_w is the vapor pressure of pure water; P_v is the vapor pressure of solution, T is the temperature; and

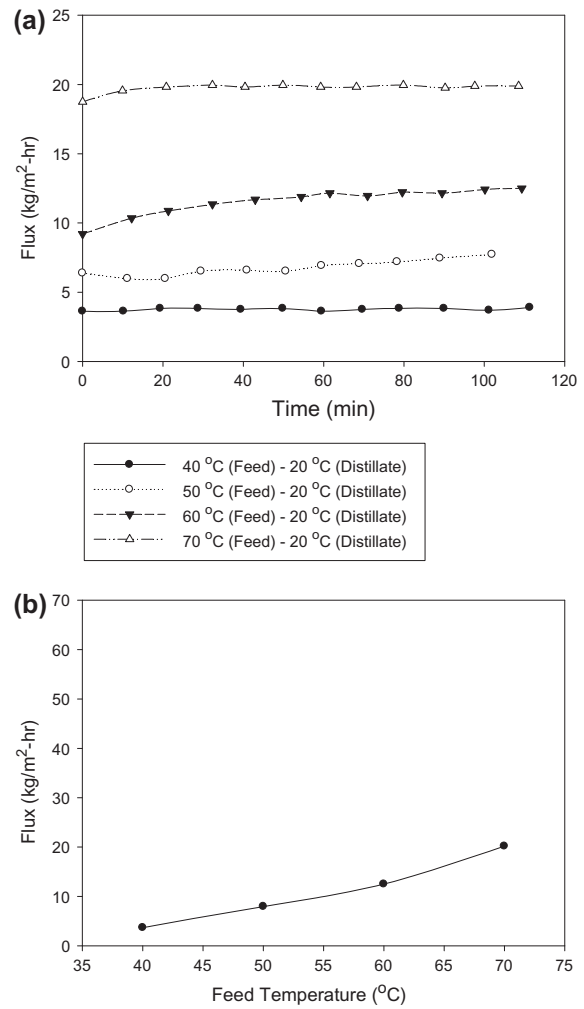


Fig. 3. Effect of feed temperature on flux in DCMD (a) flux profiles and (b) average flux.

C_m is the solute concentration. $a_1, a_2, a_3, a_4, a_5,$ and a_6 are empirical constants (for water: $a_1 = -5.8002206 \times 10^3$; $a_2 = 1.3914993$; $a_3 = -4.8640239 \times 10^2$; $a_4 = 4.1764768 \times 10^{-5}$; $a_5 = -1.4452093 \times 10^{-8}$; $a_6 = 6.5459673$). In Fig. 6, the permeate velocities for MD modules are presented as a function the vapor pressure difference. The permeate velocity was calculated from the flux. Although the feed temperature was the same, the vapor pressure differences in the VMD module are different from those in the DCMD and AGMD modules. Overall, VMD has higher vapor pressure difference than DCMD and AGMD, allowing the higher permeate velocity. In addition, DCMD and AGMD have same vapor pressure difference but different permeate velocities. These results suggest that the mass transfer in MD modules is complex and needs an in-depth analysis.

Table 2
Operating conditions of laboratory-scale MD process test unit

Item		Condition		
Operation type		DCMD	AGMD	VMD
Operation time		100 min	100 min	100 min
Effective membrane area		12.2 cm ²	12.2 cm ²	12.2 cm ²
Flow rate	Feed	24 L/h	24 L/h	24 L/h
	Permeate	24 L/h	–	–
Membrane	PVDF	0.22 μm	0.22 μm	0.22 μm
Solution	Feed (volume)	0.2 M NaCl (2L)	0.2 M NaCl (2L)	0.2 M NaCl (2L)
	Permeate	D.I water	–	–
Temperature	Feed	40, 50, 60, 70 °C	40, 50, 60, 70 °C	40, 50, 60, 70 °C
	Permeate	20 °C	–	–
Vacuum pressure	Feed	–	–	–
	Permeate	–	–	3, 100 mbar
Air gap length		–	2 mm	–

3.5. Theoretical approach of mass transfer in MD modules

To analyze the mass transfer phenomena in MD modules, a simple theoretical approach was applied. The mass transfer in MD consists of two steps: one is across the boundary layer at the feed side; the other is across the membrane. The latter is somewhat complicated and includes several basic mechanisms. Fig. 7 illustrates the relationship of all the possible basic mass transfer mechanisms; Knudsen diffusion, molecular diffusion, Poiseuille flow, and additional term (including boundary layer mass transfer and/or air gap mass transfer, etc.).

The mass transfer coefficient for molecular diffusion (B_m) is given by:

$$B_m = \frac{M_v}{1 - x_A} \frac{\varepsilon D}{\delta \tau R T_{avg}} \quad (3)$$

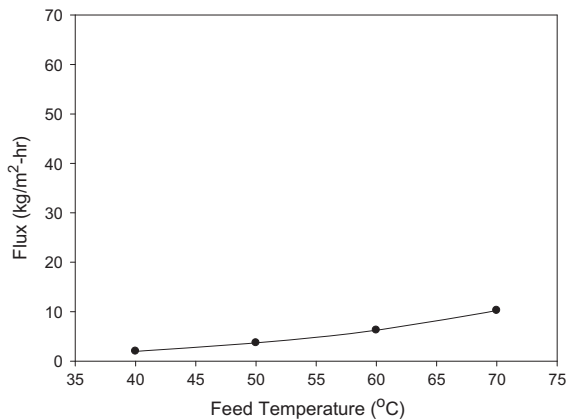


Fig. 4. Effect of feed temperature on flux in AGMD.

where M_v is the molecular weight; x_A is the mole fraction of water vapor; ε is the porosity of the membrane; δ is the membrane thickness; τ is the pore tortuosity; R is the gas constant; and T_{avg} is the average temperature inside the membrane pore; and D is the diffusivity in the pores, which can be described by:

$$D = \frac{1.895 \times 10^{-5} T^{2.072}}{P} \quad (4)$$

The mass transfer coefficient for Knudsen diffusion (B_k) is given by:

$$B_k = 1.064 \frac{r \varepsilon}{\delta \tau} \sqrt{\frac{M_v}{R T_{avg}}} \quad (5)$$

where r is the membrane pore size.

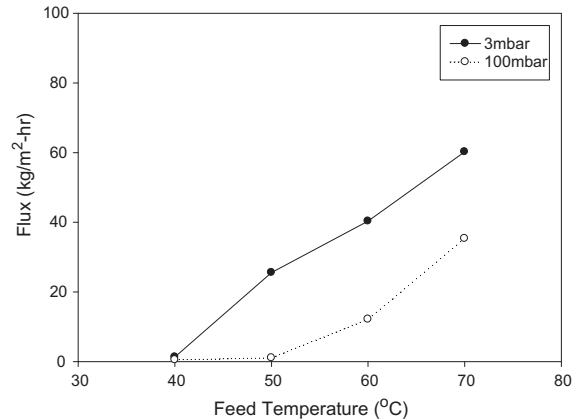


Fig. 5. Effect of feed temperature on flux in VMD.

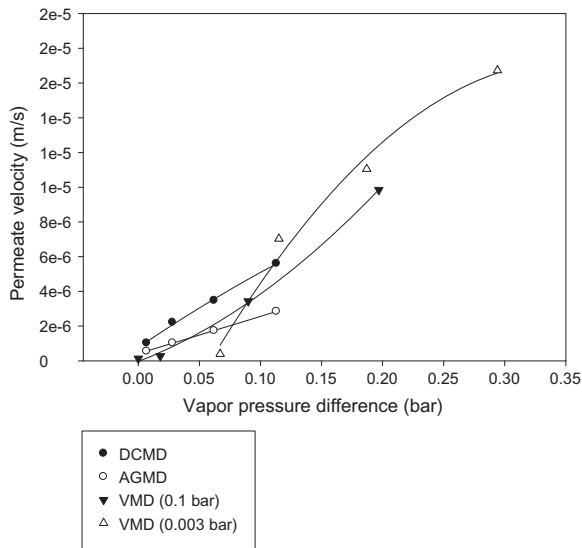


Fig. 6. Dependence of permeate velocity on vapor pressure difference across the membrane.

The mass transfer coefficient for Poiseuille flow (B_v) is given by:

$$B_v = \frac{r^2 \epsilon M_v}{\delta \tau} \frac{P_m}{8 \eta R T} \quad (6)$$

where η is the vapor viscosity and P_m is the pressure inside the pore.

Finally, the mass transfer coefficient for additional transport (B_l is calculated by):

$$N_l = \frac{1}{\frac{1}{N_{exp}} - \frac{1}{N_{sum}}} \quad (7)$$

$$B_l = \frac{N_l}{\Delta P} \quad (8)$$

where N_l is the flux by additional transport mechanism; N_{exp} is the flux determined by the experiments;

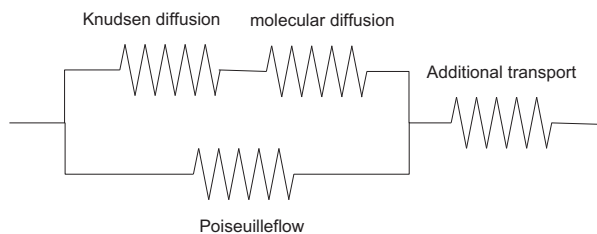


Fig. 7. Schematic representation of mass transfer in MD.

ΔP is the vapor pressure difference; and N_{sum} is the overall flux by the three mechanisms (molecular diffusion, Knudsen diffusion; and Poiseuille flow). Note that the additional mass transfer coefficient is empirically determined. All kinds of mass transfer losses can be considered through this approach.

The occurrence and the weight of a mechanism in mass transfer process rest on the characteristics and structure of the membrane module. For instance, the contribution of Poiseuille flow is negligible for DCMD and AGMD. On the other hand, the molecular diffusion is negligible for VMD. The relative contribution of transport mechanisms may depend on the module type as well as operating conditions. Finally, B_t is given by:

$$B_t = \frac{1}{\frac{1}{B_m} + \frac{1}{B_k} + \frac{1}{B_l}} \quad \text{for DCMD and AGMD}$$

$$B_t = \frac{1}{\frac{1}{B_m+B_v} + \frac{1}{B_l}} \quad \text{for VMD}$$

Fig. 8 shows the mass transfer coefficients by different mechanisms in the DCMD module. The mass transfer coefficient for Knudsen diffusion is the highest and that for additional transport is the lowest. This implies that there are additional losses in mass transfer in the current DCMD module, which may result from boundary layer resistance and temperature

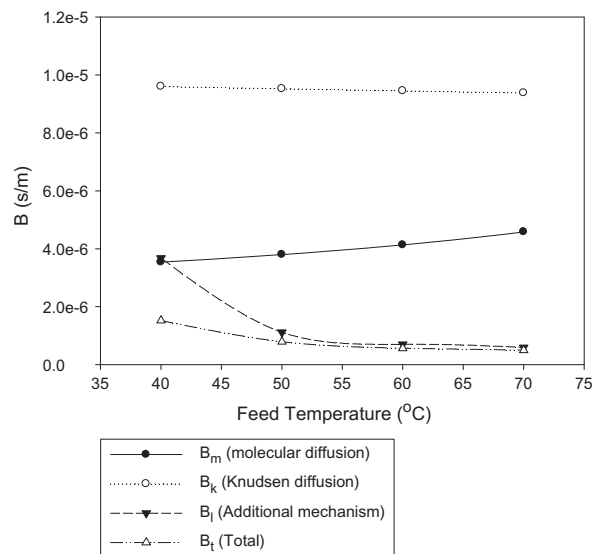


Fig. 8. Comparison of membrane mass transfer coefficients by different mechanisms in DCMD.

polarization. Compared with Knudsen diffusion, the molecular diffusion was small. In this case, the mean free path was calculated to about 0.11 μm and the Knudsen number is 0.268, which is large enough to make the Knudsen diffusion dominant.

Fig. 9 shows the mass transfer coefficients according to different mechanisms for the AGMD module. Compared with DCMD, the mass transfer coefficient is smaller, which is attributed to additional mass transfer resistance by the air gap. In fact, the additional mass transfer coefficient is much smaller in AGMD, leading to a decrease in the overall mass transfer coefficient.

The results for VMD are shown in Fig. 10(a) and (b). In VMD, the mass transfer by viscous flow is considered instead of molecular diffusion. Regardless of the degree of vacuum, the Knudsen diffusion is the fastest mass transfer mechanism. However, the overall mass transfer is limited by additional mass transfer resistance, which may result from mass transfer from the module to the condenser and vapor condensation in the condenser. If this additional resistance is reduced, higher flux may be obtained in VMD. At high degree of vacuum (Fig. 10(b)), the B_l is higher than that at low degree of vacuum (Fig. 10(a)), implying that the degree of vacuum may affect the additional mass transfer resistance.

Fig. 11 compares the dependence of the overall mass transfer coefficients on temperature in different MD modules. The overall mass transfer coefficient

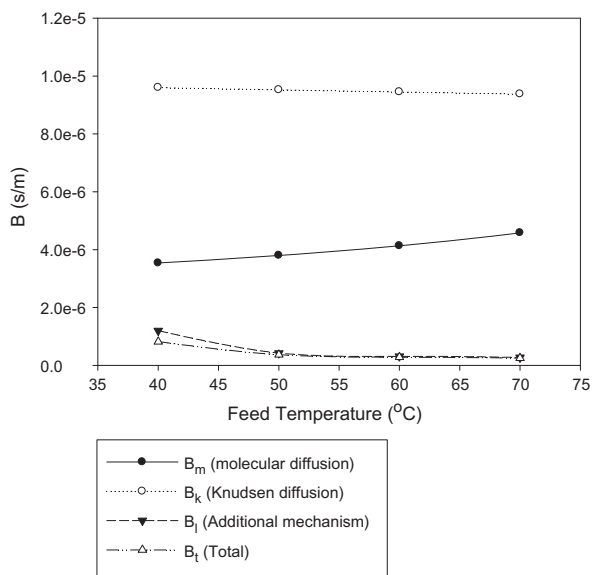


Fig. 9. Comparison of membrane mass transfer coefficients by different mechanisms in AGMD.

decreases with increasing temperature in DCMD and AGMD; while it increases with temperature in VMD. This suggests that the mass transfer efficiency is proportional to feed water temperature in VMD and inversely proportional in DCMD and AGMD. However, the flux increases with temperature even in DCMD and AGMD because the increasing rate of vapor pressure with temperature is higher than the decreasing rate of mass transfer coefficients. These results indicate that the operating conditions such as

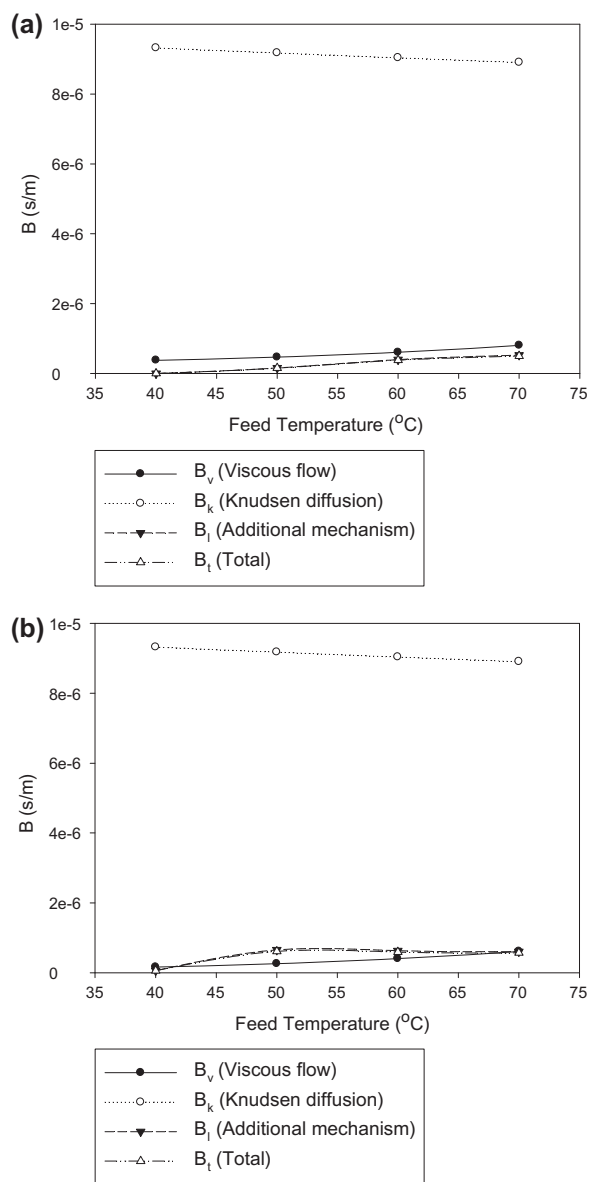


Fig. 10. Comparison of membrane mass transfer coefficients by different mechanisms in VMD (a) 100 mbar vacuum and (b) 3 mbar vacuum.

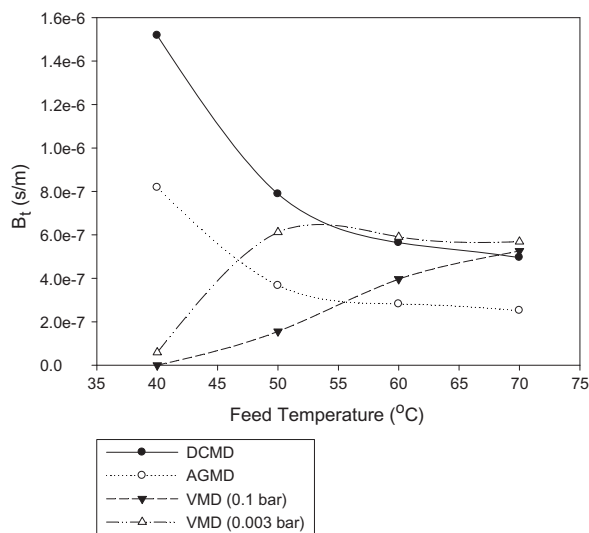


Fig. 11. Dependence of total membrane mass transfer coefficients for different MD modules on feed temperature.

feed temperature should be determined by considering not only flux and productivity but also mass transfer coefficient.

4. Conclusions

In this work, three MD modules including DCMD, AGMD, and VMD were compared to provide insight into the design and optimization of MD systems. The following conclusions can be drawn:

- (1) Although the same membrane was used under similar operating conditions, the flux was different, which is attributed to the difference in the transport mechanism. The flux in VMD at high degree of vacuum was the highest and that in AGMD was the lowest. The flux in VMD was highly affected by the change in feed temperature.
- (2) Under the test conditions, the Knudsen diffusion was the fastest. However, due to additional mass resistance, the overall mass transfer was much lower. Molecular diffusion was smaller than Knudsen diffusion in DCMD and AGMD. Poiseuille flow effect was negligible in VMD.
- (3) In DCMD and AGMD, the overall mass transfer coefficient decreases with increasing temperature. However, in VMD, it increases with temperature. Accordingly, DCMD and AGMD

seem to be less efficient at high feed temperatures while VMD seems to be more efficient at high feed temperatures.

Acknowledgments

This research was supported by a grant (code 13IFIP-B065893-01) from Industrial Facilities & Infrastructure Research Program funded by Ministry of Land, Infrastructure and Transport of Korean government.

References

- [1] A.M. Alkhalbi, The potential of membrane distillation as a stand-alone desalination process, *Desalination* 223(1–3) (2008) 375–385.
- [2] A.M. Alkhalbi, N. Lior, Membrane-distillation desalination: Status and potential, *Desalination* 171(2) (2005) 111–131.
- [3] K.L. Hickenbottom, T.Y. Cath, Sustainable operation of membrane distillation for enhancement of mineral recovery from hypersaline solutions, *J. Membr. Sci.* 454 (2014) 426–435.
- [4] A. Alkhalidhiri, N. Darwish, N. Hilal, Membrane distillation: A comprehensive review, *Desalination* 287 (2012) 2–18.
- [5] M. Khayet, Membranes and theoretical modeling of membrane distillation: A review, *Adv. Colloid Interface Sci.* 164(1–2) (2011) 56–88.
- [6] R.B. Saffarini, E.K. Summers, H.A. Arafat, J.H. Lienhard, Economic evaluation of stand-alone solar powered membrane distillation systems, *Desalination* 299 (2012) 55–62.
- [7] J. Blanco Gálvez, L. García-Rodríguez, I. Martín-Mateos, Seawater desalination by an innovative solar-powered membrane distillation system: The MEDESOL project, *Desalination* 246(1–3) (2009) 567–576.
- [8] A. Cipollina, M.G. Di Sparti, A. Tamburini, G. Micale, Development of a membrane distillation module for solar energy seawater desalination, *Chem. Eng. Res. Design* 90(12) (2012) 2101–2121.
- [9] D. Singh, K.K. Sirkar, Desalination of brine and produced water by direct contact membrane distillation at high temperatures and pressures, *J. Membr. Sci.* 389 (2012) 380–388.
- [10] M. Khayet, T. Matsuura, J.I. Mengual, M. Qtaishat, Design of novel direct contact membrane distillation membranes, *Desalination* 192(1–3) (2006) 105–111.
- [11] M. Khayet, C. Cojocar, Air gap membrane distillation: Desalination, modeling and optimization, *Desalination* 287 (2012) 138–145.
- [12] M. Khayet, C. Cojocar, A. Baroudi, Modeling and optimization of sweeping gas membrane distillation, *Desalination* 287 (2012) 159–166.
- [13] J. Zhang, J.-D. Li, M. Duke, M. Hoang, Z. Xie, A. Groth, C. Tun, S. Gray, Modelling of vacuum membrane distillation, *J. Membr. Sci.* 434 (2013) 1–9.

- [14] M. Khayet, T. Matsuura, Membrane distillation hybrid systems, in: M. Khayet, T. Matsuura (Eds.), *Membrane Distillation*, chapter 14, Elsevier, Amsterdam, 2011, pp. 399–427.
- [15] H. Geng, H. Wu, P. Li, Q. He, Study on a new air-gap membrane distillation module for desalination, *Desalination* 334(1) (2014) 29–38.
- [16] C.-K. Chiam, R. Sarbatly, Vacuum membrane distillation processes for aqueous solution treatment—A review, *Chem. Eng. Process.* 74 (2013) 27–54.
- [17] M. Qtaishat, T. Matsuura, B. Kruczek, M. Khayet, Heat and mass transfer analysis in direct contact membrane distillation, *Desalination* 219(1–3) (2008) 272–292.
- [18] M. Khayet, C. Cojocaru, M.C. García-Payo, Experimental design and optimization of asymmetric flat-sheet membranes prepared for direct contact membrane distillation, *J. Membr. Sci.* 351(1–2) (2010) 234–245.